Photoionization cross section of the $4p^5 5d[7/2]\ J=4$ state and radiative lifetimes of three states of Kr I

B. D. Cannon, W. L. Glab,* and Rachel Ogorzalek-Loo
Pacific Northwest Laboratory, P.O. Box 999, Richland, Washington 99352
(Received 6 July 1992)

Three states in Kr I were studied in a pure Kr discharge at pressures ≤ 15 mTorr. Two-photon excitation from the metastable $4p^5 5s[3/2]\ J=2$ state produced the $4p^5 5d[7/2]\ J=4$ state whose photoionization cross section and lifetime were measured. The photoionization cross section at $\lambda=1064$ nm is 32 ± 5 Mb, and the radiative lifetime is 142 ± 12 ns. One-photon excitation produced the $4p^5 5p[5/2]\ J=2$ and $J=3$ states of Kr I, whose radiative lifetimes were measured. In contrast to previous lifetime measurements of these two $5p$ states, this work used both state-specific excitation and low pressures. The pressures were low enough that collisional transfer between these two states was negligible. In a very clean 8-mm-diam cell, the $5p[5/2]\ J=3$ lifetime increased with Kr pressure. This increase is attributed to radiation trapping on the $5s[3/2]\ J=2$ to $5p[5/2]\ J=3$ transition. This radiation trapping by the metastable first excited state of Kr I was observed in a pure Kr discharge at pressures below 4 mTorr.

PACS number(s): 32.70.Fw, 32.80.Fb

I. INTRODUCTION

Photoionization cross sections and radiative lifetimes of an excited state depend on the strength of the coupling of this state by photons to other states, either continuum or bound. The strengths of these couplings are of interest as fundamental parameters in atomic physics and because of important applications in astrophysics, laser physics, and laser-based elemental and isotopic analyses. Photoionization and its inverse process, radiative ion-electron recombination, can be dominant processes in outer space where collisions are rare. In multiatmosphere excimer-laser plasmas, the high concentrations of lasing photons can make photoionization the dominant loss mechanism for important precursors to the lasing species. Thus photoionization can limit the energy-extraction efficiency in these lasers. In laser-based atomic-detection techniques, such as resonance-ionization spectroscopy (RIS), photoionization cross sections and lifetimes of excited states must be known to predict the potential sensitivity and selectivity of a particular scheme. RIS is being used for an increasing range of applications [1] including spectroscopy, single-atom detection, elemental analysis, ultrasensitive isotopic analysis, plasma diagnostics in semiconductor processing, and fundamental physics experiments.

A proposed approach for ultrasensitive isotopic analysis of Kr [2] uses RIS of the metastable $5s[3/2]_{J=2}$ state. This approaches uses continuous-wave single-frequency lasers for two-color two-photon excitation to the $5d[7/2]_4$ state via the $5p[5/2]_3$ state followed by photoionization at 1064 nm (see Fig. 1). This path is predicted to be very efficient and provide high isotopic selectivity. If this approach or another [3–6] can provide the required sensitivity and selectivity, several applications using the rare radioactive isotopes ^{81}Kr and ^{85}Kr will become possible. There are several dating applications for ^{81}Kr in climatology and hydrology [7,8]. With its 2.1×10^5-yr half-life, ^{81}Kr could be used to date events on the time scale of 10^5-10^6 years. A solar-neutrino experiment that requires ultrasensitive detection of ^{81}Kr has also been proposed [9]. Applications for ^{85}Kr detection [7,8] include dating ground water less than 30 years old, atmospheric transport, and contamination of old air or water samples with modern air. The actual efficiency and selectivity of this RIS scheme depends on the photoionization cross section and radiative lifetime of $5d[7/2]_4$ state and the radiative lifetime of the $5p[5/2]_3$ state.

The first measurements of the photoionization cross sections of excited states of Kr [10] looked at the role of autoionization and determined an upper limit for the threshold photoionization cross section of the $5s$ metastable states. Later work on excited-state photoionization of Kr, both experimental [11] and theoretical [12–14], was largely prompted by the importance of these processes in excimer lasers The cross sections of the $5s[3/2]_2$ state at $\lambda=248$ nm [11] and the $6p[3/2]_2$ state at $\lambda=193$ nm [15,16] have been measured. The measurements of both these states used the coincidence between the ArF laser wavelength and the two-photon transition from the ground state to the $6p[3/2]_2$ state of Kr. This limited set of experimental data does not test many of the predictions of the calculations, for example, the prediction that threshold cross sections for p and d states are comparable and nearly two orders of magnitude larger than for the s states.

The lifetimes of the $5p$ levels in Kr have been measured many times [17–19]. An extensive compilation of lifetime measurements for the $5p$ levels in Kr can be found in [17]. These levels play important roles in energy transfer and production of the metastable $5s[3/2]_2$ state. The $5p[5/2]\ J=2$ and $J=3$ state lifetimes have been difficult to measure accurately. The cross sections for collisional equilibration between these two states separated by 13 cm^{-1} is very large ($\approx10^{-14}$ cm^2) [17]. Only at pressures

well below 100 mTorr can the radiative decay rates be cleanly separated from this collisional process. Previous measurements for these two states have suffered from either high pressures [17] or radiative cascades produced by nonselective excitation [18,19]. We report lifetimes measured using selective excitation at pressures below 15 mTorr, which are free from these problems. At 15 mTorr, the collisional transfer rates are less than 1% of the radiative rates.

II. EXPERIMENT

Time-resolved laser-induced fluorescence with wavelength-resolved detection was used in this work. Figure 1 shows a partial energy-level diagram of Kr, the excitation wavelengths in vacuum [20,21], and the photoionization process studied in this work. The photoionization cross section was determined from the depletion of the $5d[7/2]_4$ state fluorescence by the 1064-nm photoionizing laser beam. Resonant detection of the fluorescence was used for the two $5p$ states because nonresonant emission is not allowed for the $5p[5/2]_3$ state and the nonresonant emission wavelengths from the $5p[5/2]_2$ state are too long to be detected with our system. Both steps in the radiative cascade from the $5d[7/2]_4$ state to the $5s[3/2]_2$ via the $5p[5/2]_3$ state were detected because these two wavelengths were not resolved by the monochromator.

A pulsed dye laser (Lambda Physik Model FL 2002) pumped by the 532-nm output of a neodymium-doped yttrium aluminum garnet (Nd:YAG) laser (Molectron model MY 32) excited Kr in the $5s[3/2]_2$ state in a pure Kr discharge. Typical dye-laser pulse energies were 30 μJ.

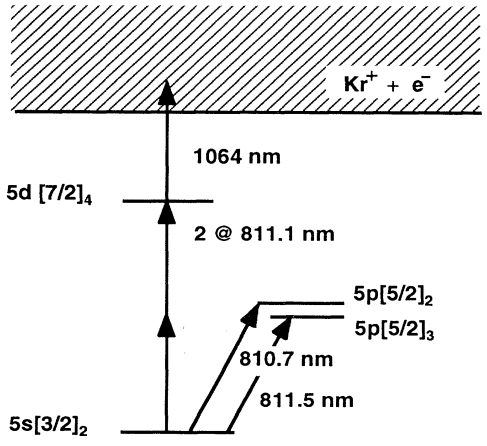

FIG. 1. Partial energy-level diagram of Kr showing the states and vacuum wavelengths of the three transitions used for excitation. The states are labeled using Racah notation, which is of the form $nl[k]_J$ where n and l are the outer electron's principal and orbital-angular-momentum quantum numbers, k is the angular-momentum quantum number of the ion core coupled with l, and J is the total electronic angular-momentum quantum number. The photoionization of the $5d[7/2]_4$ state at 1064 nm is also shown.

For the two-photon excitation, the dye-laser beam was focused with a 200-mm-focal-length lens. For one-photon transitions, there was more signal without this lens; however, focusing the dye laser had no observed effect on the lifetimes. A collection lens imaged the fluorescence onto the entrance slit of a 0.1-m-focal-length monochromator (Oriel Model 7240, bandpass typically 1 nm). The light exiting the monochromator was detected with a photomultiplier (Hamamatsu Model R928). The signals were recorded and averaged in a digital oscilloscope (Tektronix Model 2440) with a 400-MHz bandwidth and 500-MHz sampling rate. From the oscilloscope, data were transferred to a computer for scattered-light subtraction and nonlinear least-squares fitting of a single exponential decay to the data.

A radio frequency (rf) discharge produced Kr $5s[3/2]_2$ metastable states in a 20-cm-long quartz or Pyrex cell with windows sealed on with a glass frit (Vitta Corp.). These cells were made from 12-mm-o.d. tubing and sealed with all metal valves (Nupro SS-4H) connected to the cell using glass-to-metal seals. The best indication of a clean cell and high Kr purity was the ability to sustain a pure Kr discharge at less than 1 mTorr with rf powers of less than 1 W. The best cleaning procedure for the cell found in this work consisted of first baking the cell overnight at 250 °C followed by baking an additional 2 h at 360 °C while being pumped by a vacuum system with a base pressure of 2×10^{-8} Torr. Following the baking, the cell was filled with 1 Torr Kr, an rf discharge was started, and the cell was then pumped out until the discharge was extinguished. This cycle of filling, discharging, and pumping was repeated at least four times. Following this preparation, a faint discharge could be seen in the cell even when the ion gauge on the vacuum system was registering in the region of 10^{-6} Torr. The Kr used to fill the cells came from a reservoir immersed in liquid nitrogen. The Kr in this reservoir was originally from a lecture bottle (Matheson 99.95% Kr) and had been further purified by several freeze-pump-thaw cycles using liquid nitrogen. An rf discharge pumps Kr [22,23] at pressures of 60 mTorr and below with moderate speed by implanting Kr ions into the cell walls. Stable Kr pressures were obtained in sealed cells only by first running the rf discharge with the cell connected to the vacuum line. A few hours were required for the cell pressure to stabilize. Presumably a steady state was approached between the discharge implanting and releasing Kr from the cell walls.

Figure 2 shows a typical pair of fluorescence decays used for the photoionization cross-section measurements. The background from scattered dye-laser light has been subtracted from each trace. The fluorescence comes from both the $5d[7/2]_4$ state and the $5p[5/2]_3$ state that is produced by radiative decay of the $5d[7/2]_4$ state. The emissions from these two states are only partially resolved by the monochromator. Thus the time dependence of the fluorescence changes with the lifetimes of both states. After both excitation and photoionization, there are "fast" transients in the fluorescence with the $5p[5/2]_3$-state lifetime.

Pairs of fluorescence decays were recorded, with and without the 1064-nm beam going through the cell. The

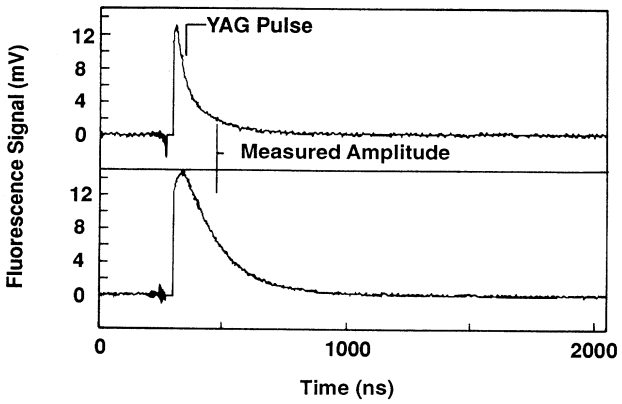

FIG. 2. Fluorescence decays from the $5d[7/2]_4$ state with (upper curve) and without (lower curve) photoionization by a 1064-nm pulse from a YAG laser with a fluence of 7×10^{16} photons/cm^2. Also shown are the timings of the YAG pulse and where the fit begins for measuring amplitudes lifetimes. The noise before the beginning of the fluorescence is from electrical noise created by the firing of the Q switch. The Kr pressure was 1 mTorr.

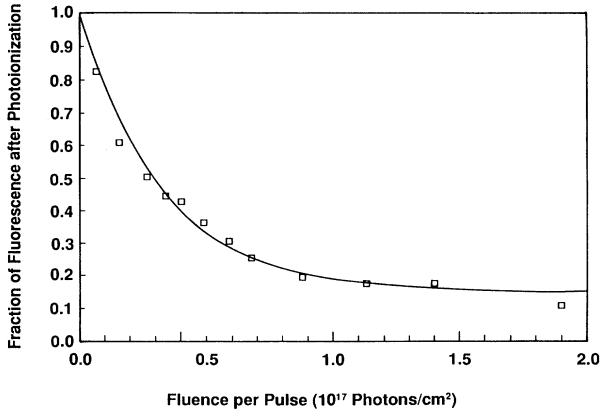

FIG. 3. Depletion of $5d[7/2]_4$-state fluorescence by photoionization at 1064 nm. Each point is the ratio of the amplitudes at the beginning of the fit of a pair of fluorescence decays like those in Fig. 2. The nonzero base line results from the $5p[5/2]_3$ population as discussed in the text.

1064-nm beam was delayed with an optical delay line to arrive in the cell 50 ns after the dye-laser pulse. After the 20 m of travel from the Nd:YAG laser to the cell, the 1064-nm beam was over 2 cm in diameter. Near the cell a 4.5-mm-diam aperture selected the portion of the 1064-nm beam that entered the cell. The 1064-nm power entering the cell was measured with a volume absorbing calorimeter (Scientech 360001). To minimize problems caused by scattered dye-laser light and "fast" transients with the lifetime of the $5p[5/2]_3$ state, both decays in the pair were fit for times longer than 140 ns after the start of the fluorescence. After the "fast" transients, the fluorescence is well fit by a single exponential decay. From a plot of the ratio of the amplitudes from the fit versus the fluence in the 1064-nm beam, the photoionization cross section was determined. The fluorescence decays without the 1064-nm beam present were used in determining the lifetime of the $5d[7/2]_4$ state.

III. RESULTS AND DISCUSSION

A. Photoionization

Figure 3 shows one set of photoionization data for the $5d[7/2]_4$ state, i.e., a plot of the amplitude ratios R from 12 pairs of decays similar to those in Fig. 2 versus the 1064-nm fluence F. The solid line is the result of a least-squares fit to these data of the function

$$R=(1-B)\exp(-\sigma F)+B\ , \tag{1}$$

where σ is the photoionization cross section and B is the base line. This base line results from the $5p[5/2]_3$-state population produced by the main radiative decay channel of the $5d[7/2]_4$ state. This state is not photoionized at 1064 nm and its emission is detected along with the main $5d[7/2]_4$ emission. The lifetime of the $5p[5/2]_3$ state and the ratio of the monochromator transmissions for the two wavelengths both affect the size of this base line. Thus B is affected by small changes in the tuning of the monochromator or changes in the Kr pressure. The pumping of Kr by the discharge can substantially change the $5p[5/2]_3$ lifetime because of radiation trapping as discussed below. Data sets used to determine the photoionization cross section were taken with the Kr pressure stabilized at 1 mTorr by running the discharge in the cell for several hours while it was on the vacuum line. The low Kr pressure minimized radiation trapping and the stable Kr pressure reduced changes in the radiation trapping during a set of measurements. Our measured photoionization cross section is 32 ± 5 Mb. The main uncertainties in the cross section are due to uncertainties in the beam profile and in the power measurement.

There are no published calculations nor measurements of photoionization cross sections of the Kr $5d$ levels for direct comparison. Calculations for the $4d$ levels of Kr and $5d$ levels of Xe [14] give photoionization cross sections of 20 and 30 Mbarn, respectively, at the same photoelectron energy as in this work, 0.2 eV. These calculations [12,14] use a single-particle central-field approximation. They only consider the electron configuration and average over the fine-structure states, which have different total angular momenta and energies. Only the outer electron's principal quantum number and orbital angular momentum are included in this treatment. The two-fine-structure states of the Kr and Xe ion cores are also neglected. Thus this treatment neglects autoionization, which in the rare gases is built upon the $^2P_{1/2}$ fine-structure component of the ion core.

Autoionizing resonances are not important for the photoionization cross section of the $5d[7/2]_4$ state at $\lambda=1064$ nm. The nearest known Kr autoionizing resonance that is allowed by angular-momentum selection rules from the $5d[7/2]_4$ state is the $5f'[5/2]_3$ state [10]. This autoionizing resonance has a linewidth of less than

18 cm^{-1} and is 160 cm^{-1} off resonance at 1064 nm. This f' autoionization series is well fit by a simple extrapolation of the f' Rydberg series with small quantum defects ($\sim 10^{-2}$) [10]. The other autoionizing states accessible from the $5d[7/2]_4$ state have $J=3$, 4, or 5 and $l \geq 2$. These states should all have small quantum defects [24] and thus be close to the $5f'$ $J=3$ series. The linewidths of these high-J and -l autoionizing states also should be narrow because the outer electron is weakly coupled to the ion core [10,26]. Thus neglect of autoionizing resonances should be a good approximation in calculations of the cross section of the $5d[7/2]_4$ state at $\lambda = 1064$ nm.

Within the approximation of neglecting the details of the ion core, we also can compare our results to calculations on Rb. This is analogous to the comparisons made in [14] between the calculated photoionization cross sections of Xe*($5d$) and Cs*($5d$). The similarities in the photoioization cross sections are reasonable because the $5d$ electron is well outside the ion core and the ion cores are similar in structure [14]. A threshold photoionization cross section of 40 Mb was calculated [25] for the $5d$ levels of Rb using the single-particle central-field approximation. These values are in good agreement with our result for the $5d[7/2]_4$ state of Kr given the differences between what was calculated and what we measured.

A calculation that treats individual total angular-momentum states and autoionizing states could be done using multichannel-quantum-defect theory as was done in recent theoretical studies of multiphoton ionization of Kr and Xe [26,27]. Unfortunately, this work did not include states with $J \geq 4$, and excited-state photoionization cross sections were not published.

B. Radiative lifetimes

The radiative lifetimes of the $5d[7/2]_4$ state and the two $5p$ states measured in this work are shown in Table I with other results in the literature. The error estimates for our lifetimes are one standard deviation of the measurements. The $5d[7/2]_4$ lifetimes were determined from decays with no 1064-nm laser beam present. The radiative lifetime we report for this state is the average of 89 measurements. These 89 measurements include some data from "early" experiments conducted before we learned of the pumping of Kr by the discharge. The pumping of Kr by the discharge means the real pressure was much less than the initial pressure. This data from our early work had the cell initially filled with less than 60 mTorr of Kr. "Later" data was taken at pressures of 15 mTorr or less but with the pressure stabilized by running the discharge with the cell attached to the vacuum system. No pressure dependence is observed in these lifetimes in this pressure range. Our result for this lifetime is bracketed by the two values calculated in [28].

TABLE I. Radiative lifetimes (ns) of the three states of Kr studies in this work. The numbers in parentheses are the error estimates of the last digits shown. For this work the error estimates are one standard deviation of the measurements. Results of others for these lifetimes, both experimental and theoretical, are also given. An extensive compilation of results for the $5p$ states is given in [17].

State	This work	Refs. Ref. [17]	[18] and [19]	Ref. [28]
$5p[5/2]_3$	30.2(14)	28.7(20)	31.0(30)	22.4[a] 29.7[b]
$5p[5/2]_2$	32.5(8)	26.5(20)	32.1(15)	26.5[a] 31.4[a]
$5d[7/2]_4$	142.0 (12)			132[a] 169[b]

[a]Length formulation of dipole-moment operator.
[b]Velocity formulation of the dipole-moment operator. The difference between the length and velocity formulations gives an estimate of the error in these calculations.

Figure 4 shows a plot of the lifetime of the $5p[5/2]_3$ state versus Kr pressure. The data plotted at 0 mTorr represent five early measurements with initial fill pressures ranging from less than 10 to 60 mTorr. These lifetimes were independent of initial pressure to within the experimental error. The fluorescence intensities in these early measurements are consistent with a metastable $5s[3/2]_2$ state population more than an order of magnitude lower than in the data set represented by the 1-mTorr point in Fig. 4. The points in Fig. 4 at pressures above zero were taken with the pressure stabilized and with improved cleaning and purification procedures. The intercept of a least-squares line through the nonzero pressure data agrees with the average of the "early" data. The radiative lifetime we report for this state and the solid line in Fig. 4 is from a linear least-squares fit to all the data shown in Fig. 4. Our $5p[5/2]_2$ lifetime is the average of six measurements corresponding to the data in Fig. 4 plotted at 0 mTorr. No dependence on initial fill pressure was observed in this data. This transition is less prone to radiation trapping because of the smaller absorption cross section and because of the large (75%) branching to the $5s[3/2]_1$ state [17].

Our results for the lifetimes of the $5p[5/2]_3$ and

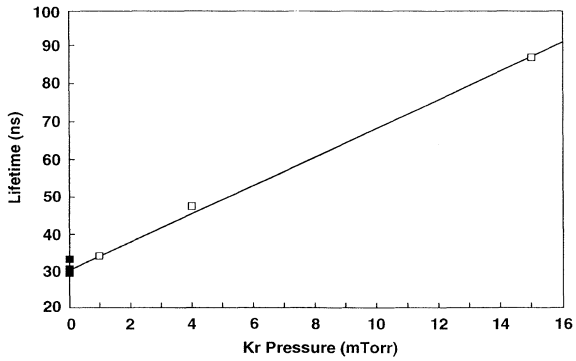

FIG. 4. Lifetimes of the $5p[5/2]_3$ state vs Kr pressure. The points plotted at 0 mTorr were taken with concentrations of the $5s[3/2]_2$ state at least an order of magnitude lower than the 1-mTorr point as determined from the amplitudes of the fluorescence signals. See text for full explanation.

$5p[5/2]_2$ states are in excellent agreement with those reported in [18,19] that were measured at pressures between 1 and 50 mTorr using pulsed electron-beam excitation. Radiative cascades into these levels seem to have been adequately modeled with their multiexponential fits. The results of [17] for these two states are a little lower than our values, although only for the $5p[5/2]_2$ state does the difference exceed the combined error estimates. The measurements in [17] used laser excitation of Kr $5s[3/2]_2$ in an Ar buffer gas between 1 and 10 Torr. While the excitation in [17] was state selective, the high Ar buffer gas pressures required use of a model for analyzing their data that included collisional transfer between and radiative decay of both these states. The authors in [17] say their $5p[5/2]_2$ lifetime may be too low because they could not work at lower Ar pressures. The lifetimes calculated in [28] using the velocity formulation of the dipole moment operator are in very good agreement with experiment.

Figure 4 shows that the observed lifetimes of the $5p[5/2]_3$ state in a well-cleaned cell increase with Kr pressure between 0 and 15 mTorr. The rate of increase is 3.9 ± 0.1 ns/mTorr. There are three mechanisms by which observed lifetimes can increase with pressure: (i) diffusion or free flight out of the observation region, (ii) diffusion to walls where deactivation occurs, and (iii) radiation trapping. With thermal velocities, the average distance traveled by a Kr atom in 100 ns is 30 μm, which excludes the first two mechanisms. Assuming the lifetime increase is caused by radiation trapping, we can estimate the fraction of the Kr atoms that are in the metastable state. The radiation trapped lifetime τ can be expressed [29] as $\tau/\tau_{rad}=1/(1-x)$, where $\tau_{\rm rad}$ is the radiative lifetime and $(1-x)$ is given by [30]

$$(1-x)=\left[\frac{1}{\pi}\right]^{1/2}\int_{-\infty}^{+\infty}\exp(-\omega^2)\times\exp[-\sigma_0 NL\exp(-\omega^2)]d\omega\ , \tag{2}$$

where σ_0 is the line-center Doppler-broadened absorption cross section, N is the lower-state number density, and L is the path length. This integral has been tabulated [31]. Using

$$\sigma_0=\frac{2}{\Delta\nu_D}\left[\frac{\ln 2}{\pi}\right]^{1/2}\frac{\lambda^2}{8\pi}\frac{g_2}{g_1}\frac{1}{\tau_{\rm rad}}\ , \tag{3}$$

where $\Delta\nu_D$ is the Doppler width, λ is the wavelength, and g_2/g_1 is the ratio of degeneracies, we calculate $\sigma_0=2.3\times10^{-11}$ cm^2 for this transition. Using $L=4$ mm (the inside radius of the cell) we calculate the fraction of the total Kr in the $5s[3/2]_2$ state as 5×10^{-4}.

This calculation is not a precise determination of the fraction of metastables in the discharge. This approach neglects several factors whose effects are small in this situation. The combination of the low average number of absorptions and the small collection solid angle justify neglecting the exact geometry. The predominance of three isotopes (82Kr, ^{84}Kr, and ^{86}Kr comprise 86% of natural Kr) whose isotope shifts ($\approx$65 MHz) [32] are much smaller than the Doppler width (500 MHz) justifies using only a single Doppler-broadened line in this treatment. This calculation does show that radiation trapping is a likely explanation of the observed increase in lifetime with pressure since the calculated metastable fraction is a reasonable number.

IV. CONCLUSION

The measurement of the photoionization cross section of a $5d$ state of Kr is in good agreement with the calculations on similar systems. With a photoelectron energy of 0.2 eV, we measured essentially the threshold cross section for the $5d[7/2]_4$ state. It is interesting to compare the cross section from this work with experimental results for the $5s$ states. At threshold, a value of ≤0.49 Mb has been reported [10] and at 0.9 eV above threshold the cross section is 0.51 ± 0.11 Mb [11]. These results support the trend predicted by the calculations of [14] that threshold photoionization cross sections increase by two orders of magnitude in going from s to d electrons. Calculations on Rb [33] show that this is unlikely to be an effect of the principal quantum number. This is in contrast to atomic hydrogen, where the threshold photoionization cross sections are independent of l [33].

The agreement between our measured $5d[7/2]_4$ radiative lifetime and that calculated in [28] supports the accuracy of these calculations for the $5d$ levels in Kr. This agreement also supports the accuracy of these calculations for the $5d$ levels in Kr. This agreement also supports the accuracy of the calculated radiative rates from the $5d[7/2]_4$ state. These calculated rates predict that in the absence of collisions and photoionization, greater than 90% of the atoms in the $5d[7/2]_4$ state radiatively cascade into the metastable $5s[3/2]_2$ state. The low loss rate, the narrow natural linewidth (1.1 MHz), the efficient two-color two-photon excitation, and the large photoionization cross section at $\lambda=1064$ nm make the $5d[7/2]_4$ state an attractive intermediate for RIS of Kr using continuous-wave lasers.

The radiative lifetimes of the two $5p[5/2]$ states measured in this work are free from the uncertainties of collisional transfer between these two levels and nonselective excitation. The observed lengthening of the $5p[5/2]_3$ lifetime by radiation trapping may also provide an explanation for the long lifetimes that have been reported for this state that include values as high as 59 ns [34].

ACKNOWLEDGMENTS

This work was sponsored at Pacific Northwest Laboratory by the Director, Office of Basic Energy Sciences, Chemical Sciences Division of the U.S. Department of Energy under Contract No. DE-AC06-76RLO 1830. Pacific Northwest Laboratory is operated for the U.S. Department of Energy by Battelle Memorial Institute.

*Present address: Physics Department, M.S. 1051, Texas Technical University, Lubbock, Texas 79409.

[1] See *Resonance Ionization Spectroscopy 1988,* edited by T. B. Lucatorto and J. E. Parks, IOP Conf. Proc. No. 94 (Institute of Physics and Physical Society, Bristol, 1988); *Resonance Ionization Spectroscopy 1990,* edited by J. E. Parks and N. Omenetto, IOP Conf. Proc. No. 118 (Institute of Physics and Physical Society, Bristol, 1990).

[2] B. D. Cannon and G. R. Janik, in *Resonance Ionization Spectroscopy 1988,* edited by T. B. Lucatorto and J. E. Parks, IOP Conf. Proc. No. 94 (Institute of Physics and Physical Society, Bristol, 1988).

[3] B. D. Cannon and T. J. Whitaker, Appl. Phys. B **38**, 57 (1985).

[4] J. J. Snyder, T. B. Lucatorto, P. H. Debenham, and S. Geltman, J. Opt. Soc. Am. B **2**, 1497 (1985).

[5] W. M. Fairbank, Jr., Nucl. Instrum. Methods B **29**, 407 (1987).

[6] N. Thonnard, R. D. Willis, M. C. Wright, W. A. Davis, and B. E. Lehmann, Nucl. Instrum. Methods B **29**, 398 (1987).

[7] B. E. Lehmann and H. H. Loosli, in *Resonance Ionization Spectroscopy 1984,* edited by G. S. Hurst and M. G. Payne, IOP Conf. Proc. No. 71 (Institute of Physics and Physical Society, Bristol, 1984).

[8] R. D. Willis, N. Thonnard, M. C. Wright, B. E. Lehmann, and D. Rauber, in *Resonance Ionization Spectroscopy 1988,* edited by T. B. Lucatorto and J. E. Parks, IOP Conf. Proc. No. 94 (Institute of Physics and Physical Society, Bristol, 1988).

[9] G. S. Hurst, C. H. Chen, S. D. Kramer, Raymond Davis, Jr., Bruce Cleveland, Fletcher Gabbard, and F. J. Schima, Phys. Rev. Lett. **53**, 1116 (1984).

[10] F. B. Dunning and R. F. Stebbings, Phys. Rev. A **9**, 2378 (1974).

[11] D. B. Geohegan, A. W. McGown, and J. G. Eden, J. Chem. Phys. **86**, 577 (1987).

[12] H. A. Hyman, Appl. Phys. Lett. **31**, 14 (1977).

[13] T. W. Hartquist, J. Phys. B **14**, 2101 (1978).

[14] C. Duzy and H. A. Hyman, Phys. Rev. A **22**, 1878 (1980).

[15] Jeffrey Boker, Joshua Zavelovich, and Charles K. Rhodes, Phys. Rev. A **21**, 1453 (1980).

[16] D. B. Geohegan, A. W. McGowan, and J. G. Eden, Phys. Rev. A **33**, 269 (1986).

[17] R. S. F. Chang, H. Horiguchi, and D. W. Setser, J. Chem. Phys. **73**, 778 (1980).

[18] M. V. Fonseca and J. Campos, Phys. Rev. A **17**, 1080 (1978).

[19] Victoria Fonseca and José Campos, J. Phys. B **13**, 3957 (1980).

[20] Victor Kaufman and Curtis J, Humphreys, J. Opt. Soc. Am. **59**, 1614 (1969).

[21] C. E. Moore, *Atomic Energy Levels,* Natl. Bur. Stand. (U.S.) Circ. No. 467 (U.S. GPO, Washington, DC, 1952), Vol. 2.

[22] H. S. Butler and G. S. Kino, Phys. Fluids **6**, 1346 (1963).

[23] A. O. R. Cavaleru, D. G. Armour, and G. Carter, Vacuum **22**, 321 (1972).

[24] D. Kleppner, Michael G. Littman, and Myron L. Zimmerman, in *Rydberg States of Atoms and Molecules,* edited by R. F. Stebbings and F. B. Dunning (Cambridge University Press, New York, 1983).

[25] M. Aymar, O. Robaux, and S. Wane, J. Phys. B **17**, 993 (1984).

[26] A. L'Huillier, X. Tang, and P. Lambropoulos, Phys. Rev. A **39**, 1112 (1989).

[27] X. Tang, P. Lambropoulos, Anne L'Huillier, and S. N. Dixit, Phys. Rev. A **40**, 7026 (1989).

[28] M. Aymar and M. Coulombe, At. Data Nucl. Data Tables **21**, 537 (1978).

[29] E. Matthias, R. A. Rosenberg, E. D. Poliakoff, M. G. White, S.-T. Lee, and D. A. Shirley, Chem. Phys. Lett. **52**, 239 (1977).

[30] M. I. D'yakanov and V. I. Perel, Zh. Eksp. Teor. Fiz. **47**, 1483 (1964) [Sov. Phys. JETP **20**, 997 (1965)].

[31] A. C. G. Mitchell and M. W. Zemansky, *Resonance Radiation and Excited Atoms* (Cambridge University Press, Cambridge, England, 1934), p. 323.

[32] B. D. Cannon and G. R. Janik, Phys. Rev. A **42**, 397 (1990).

[33] M. Aymar, O. Robaux, and S. Wane, J. Phys. B **17**, 993 (1984).

[34] A. Pery-Thorne and J. E. Chamberlain, Proc. Phys. Soc. London, Sect. A **82**, 133 (1976).